

Available online at www.sciencedirect.com



Trans. Nonferrous Met. Soc. China 18(2008) 857-864

Transactions of Nonferrous Metals Society of China

www.csu.edu.cn/ysxb/

Influences of stoichiometric ratio B/A on structures and electrochemical behaviors of La_{0.75}Mg_{0.25}Ni_{3.5}M_x (M=Ni, Co; x=0-0.6) hydrogen storage alloys

ZHANG Yang-huan(张羊换)^{1,2}, DONG Xiao-ping(董小平)^{1,3}, ZHAO Dong-liang(赵栋梁)¹, GUO Shi-hai(郭世海)¹, QI Yan(祁 焱)¹, WANG Xin-lin(王新林)¹

- 1. Department of Functional Materials Research, Central Iron and Steel Research Institute, Beijing 100081, China;
 - 2. School of Materials, Inner Mongolia University of Science and Technology, Baotou 014010, China;
 - 3. School of Materials Science and Engineering, University of Science and Technology Beijing, Beijing 100083, China

Received 24 September 2007; accepted 7 January 2008

Abstract: In order to investigate the influences of the stoichiometric ratio of B/A (A: gross A-site elements, B: gross B-site elements) and the substitution of Co for Ni on the structures and electrochemical performances of the AB_{3.5-4.1}-type electrode alloys, the La-Mg-Ni-Co system La_{0.75}Mg_{0.25}Ni_{3.5}M_x (M=Ni, Co; x=0, 0.2, 0.4, 0.6) alloys were prepared by induction melting in a helium atmosphere. The structures and electrochemical performances of the alloys were systemically measured. The results show that the structures and electrochemical performances of the alloys are closely relevant to the B/A ratio. All the alloys exhibit a multiphase structure, including two major phases, (La, Mg)₂Ni₇ and LaNi₅, and a residual phase LaNi₂, and with rising ratio B/A, the (La,Mg)₂Ni₇ phase decreases and the LaNi₅ phase increases significantly. When ratio B/A=3.7, the alloys obtain the maximum discharge capacities. The high rate discharge(HRD) capability of the alloy (M=Ni) monotonously rises with growing B/A ratio, but that of the alloy (M=Co) first mounts up then declines. The cycle stability of the alloy (M=Co) monotonously increases with rising B/A ratio, but it first decreases slightly then increases for the alloy (M=Ni). The discharge potential of the alloy (M=Ni) declines with increasing B/A ratio (x>0.2), but for the alloy (M=Co), the result is contrary. The substitution of Co for Ni significantly ameliorates the electrochemical performances. For a fixed ratio B/A=3.7, the Co substitution enhances the discharge capacity from 365.7 to 401.8 mA·h/g, the capacity retention ratio (S_{100}) after 100 charging-discharging cycles from 50.32% to 53.26% and the HRD from 88.65% to 90.69%.

Key words: stoichiometric ratio; La-Mg-Ni-Co alloy; hydrogen storage alloy; substitution; Co; Ni

1 Introduction

Recently, R-Mg-Ni-based (where R is a rare earth or Y, Ca) PuNi₃-type alloys have been considered to be the most promising candidate owing to their high discharge capacities (360–410 mA·h/g) and low production costs in spite of their poor cycle stabilities. A lot of investigations on this kind of alloys have been performed in the world, and some very important results have been obtained. LIU et al[1] revealed that the La_{0.7}Mg_{0.3}(Ni_{0.85}Co_{0.15})_{3.5} alloy had a multi-phases structure, and two major phases were

found, e.g. a (La, Mg)Ni₃ phase with the PuNi₃-type rhombohedral structure in space group $R\overline{3}$ m and a LaNi₅ phase with the CaCu₅-type hexagonal structure in space group P6/mmm. KOHNO et al[2] found that the La₅Mg₂Ni₂₃-type electrode alloy La_{0.7}Mg_{0.3}Ni_{2.8}Co_{0.5} had a capacity of 410 mA·h/g, and good cycle stability during 30 charge-discharge cycles. PAN et al[3] investigated the structures and electrochemical characteristics of the La_{0.7}Mg_{0.3}(Ni_{0.85}Co_{0.15})_x (x=3.15–3.80) alloy system and obtained a maximum discharge capacity of 398.4 mA·h/g, but the cycle stability of the alloy needs to be further improved. After investigating the structure and the

electrochemical performances of the La_{0.67}Mg_{0.33}Ni_{3.0-x}-Co_x (x=0-0.75) alloys, WANG et al[4] reported that the alloy (x=0.5) obtained a maximum discharge capacity of 404.47 mA·h/g, and the addition of Co significantly improved the cycle stability of the alloys. A systemic investigation on the influence of the stoichiometric ratio B/A on the structure and electrochemical performances of the AB_{3.5-4.1}-type electrode alloys will be helpful to the development of the La-Mg-Ni system electrode alloys. Therefore, in this work, the structures and electrochemical characteristics of the La_{0.75}Mg_{0.25}Ni_{3.5}M_x (M=Ni, Co; x=0-0.6) hydrogen storage alloys were investigated, and the stoichiometric ratio B/A at which the La-Mg-Ni system electrode alloy has good integrated electrochemical performances is selected.

2 Experimental

The nominal compositions of the experimental alloys were $La_{0.75}Mg_{0.25}Ni_{3.5}M_x$ (M=Ni, Co; x=0, 0.2, 0.4, 0.6). The purity of all the component metals (La, Ni, Co, Mg) was at least 99.8%. The experimental alloys were melted in a vacuum induction furnace at a high purity helium atmosphere with a pressure of 0.04 MPa for preventing the volatilization of magnesium during the melting. A cast ingot was thus obtained by pouring the melt into a copper mould cooled by water.

The alloys were mechanically crushed and ground into the powder of < 50 μ m size for X-ray diffraction (XRD). The phase structures and compositions of the alloys were determined by X-ray diffractometer (D/max/2400). The diffraction, with the experimental parameters of 160 mA, 40 kV and 10(°)/min respectively, was performed with Cu K $_{\alpha 1}$ radiation filtered by graphite. The samples prepared by direct polish were etched with a 60% HF solution, and the morphologies of the alloys were examined by SEM.

Round electrode pellets with a diameter of 15 mm were prepared by cold pressing a mixture of 0.2 g alloy powder and carbonyl nickel powder in a mass ratio of 1:4 under a pressure of 35 MPa for 5 min. After being dried for 4 h, the electrode pellets were immersed in a 6 mol/L KOH+15 g/L LiOH solution for 24 h in order to have fully wet electrodes before the electrochemical measurement.

A tri-electrode open cell, consisting of a metal hydride electrode, a NiOOH/Ni(OH)₂ counter electrode and a Hg/HgO reference electrode, was used for testing the electrochemical performances of the experimental electrodes. The electrolyte was a 6 mol/L KOH+15 g/L LiOH solution. The voltage between the negative electrode and the reference electrode was defined as the discharge voltage. In every cycle, the alloy electrode was charged with a constant current density. After resting for

15 min, it was discharged at the same current density to -0.500 V cut-off voltage.

After the alloy electrodes were completely activated, the electrochemical impedance spectroscopy(EIS) of the alloys were measured by an advanced electrochemical system PARSTAT 2273 at 50% depth of discharge(DOD) and in the frequency range from 10 kHz to 5 MHz with an amplitude of 5 mV under the open-circuit condition. The environment temperature of the measurement was kept at 30

3 Results and discussion

3.1 Structural characteristics

The XRD patterns of the $La_{0.75}Mg_{0.25}Ni_{3.5}M_x$ (M= Ni, Co; x=0-0.6) alloys are shown in Fig.1. All the alloys hold a multiphase structure, consisting of (La, Mg)₂Ni₇ and LaNi₅ major phases as well as LaNi₂ residual phase. The lattice parameters and the phase abundances of two major phases LaNi₅ and (La, Mg)₂Ni₇ in the alloys, which were calculated from the XRD data by the software Jade 6.0, are listed in Table 1. The results indicate that the lattice constants and abundances of the alloys have significant changes with the variety of the B/A ratio. It can be clearly seen that both the parameter aand the unit cell volume of the (La,Mg)2Ni7 and the LaNi₅ phases decrease with increasing B/A ratio. However, the parameter c of the $(La,Mg)_2Ni_7$ phase decreases and that of the LaNi₅ phase increases with increasing B/A ratio. The abundance of the (La,Mg)₂Ni₇ phase reduces and that of the LaNi₅ phase increases with rising B/A ratio. When B/A ratio increases from 3.5 to 4.1, the abundance of the (La,Mg)₂Ni₇ phase drops from 74.68% to 28.53%, and that of the LaNi₅ phase mounts up from 23.04% to 71.42% for the alloy (M=Ni), and from 74.68% to 31.06% and from 23.04% to 68.91% for the alloy (M=Co), respectively. The substitution of Co for Ni increases the abundance of the (La,Mg)₂Ni₇ phase but decreases that of the LaNi₅ phase, and it enlarges the lattice parameters and the cell volume of the major phases in the alloy.

The SEM images of the La_{0.75}Mg_{0.25}Ni_{3.5}M_x (M=Ni, Co; x=0–0.6) alloys are shown in Fig.2. The result obtained by energy dispersive spectrometry(EDS) (Fig.3) indicates that the experimental alloys are of multiphase structure, containing (La,Mg)₂Ni₇ (denoted by A) and LaNi₅ (denoted by B) phases, which is in agreement with the results analyzed by XRD. Because the amount of the LaNi₂ phase in the alloys is small and it attaches itself to the (La, Mg)₂Ni₇ phase in the process of growing, it is difficult to observe the morphology of the LaNi₂ phase. It is also seen in Fig.2 that the amount of the LaNi₅ phase significantly increases with increasing B/A ratio.

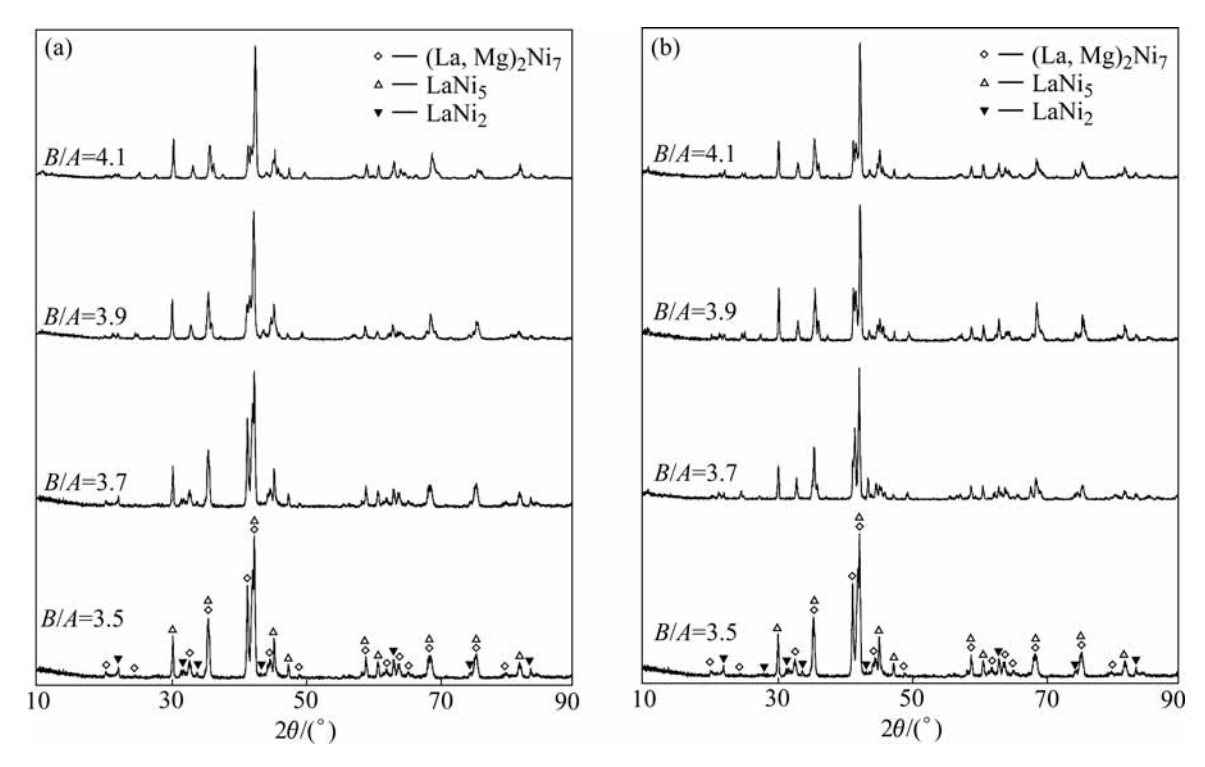


Fig.1 XRD patterns of $La_{0.75}Mg_{0.25}Ni_{3.5}M_x$ (M=Ni, Co; x=0-0.6) alloys: (a) M=Ni; (b) M=Co

Table 1 Lattice parameters and abundances of LaNi₅ and (La,Mg)Ni₃ phases

Alloy		Major phase	Lattice constant		Cell volume/	Phase aboundance
			a/nm	c/nm	nm^3	(mass fraction)/%
M=Ni	B/A=3.5	(La, Mg)Ni ₃	0.502 4	2.483 8	0.5429 2	74.68
		LaNi ₅	0.489 1	0.397 7	0.0823 9	23.04
	B/A=3.7	(La, Mg)Ni ₃	0.501 5	2.476 5	0.5393 8	61.51
		LaNi ₅	0. 481 1	0.400 2	0.0802 3	37.29
	B/A=3.9	(La, Mg)Ni ₃	0.501 2	2.469 3	0.5371 7	39.44
		LaNi ₅	0.480 1	0.401 0	0.0800 4	59.76
	B/A=4.1	(La, Mg)Ni ₃	0.500 7	2.453 4	0.5326 5	28.53
		LaNi ₅	0.478 1	0.401 6	0.0795 0	71.42
M=Co	B/A=3.5	(La, Mg)Ni ₃	0.502 4	2.483 8	0.5429 2	74.68
		LaNi ₅	0.489 1	0.397 7	0.0823 9	23.04
	B/A=3.7	(La, Mg)Ni ₃	0.501 8	2.480 6	0.5409 2	63.07
		LaNi ₅	0.484 3	0.400 8	0.0814 1	36.03
	B/A=3.9	(La, Mg)Ni ₃	0.501 7	2.473 2	0.5391 0	42.45
		LaNi ₅	0.483 0	0.402 1	0.0812 4	56.95
	B/A=4.1	(La, Mg)Ni ₃	0.501 0	2.465 2	0.5358 5	31.06
		LaNi ₅	0.482 1	0.402 7	0.0810 5	68.91

3.2 Electrochemical performances

3.2.1 Discharge potential characteristic and discharge capacity

The discharge performances are characterized by the potential plateau of the discharge curve of the alloy. The longer and the more horizontal the potential plateau, the better the potential characteristics of the alloy. The discharge potential curves of the $La_{0.75}Mg_{0.25}Ni_{3.5}M_x$ (M=Ni, Co; x=0-0.6) alloys are presented in Fig.4. It is shown that the variety of B/A ratio exerts a significantly impact on the discharge potential characteristics of the alloys. For the alloy (M=Ni), the discharge potential of

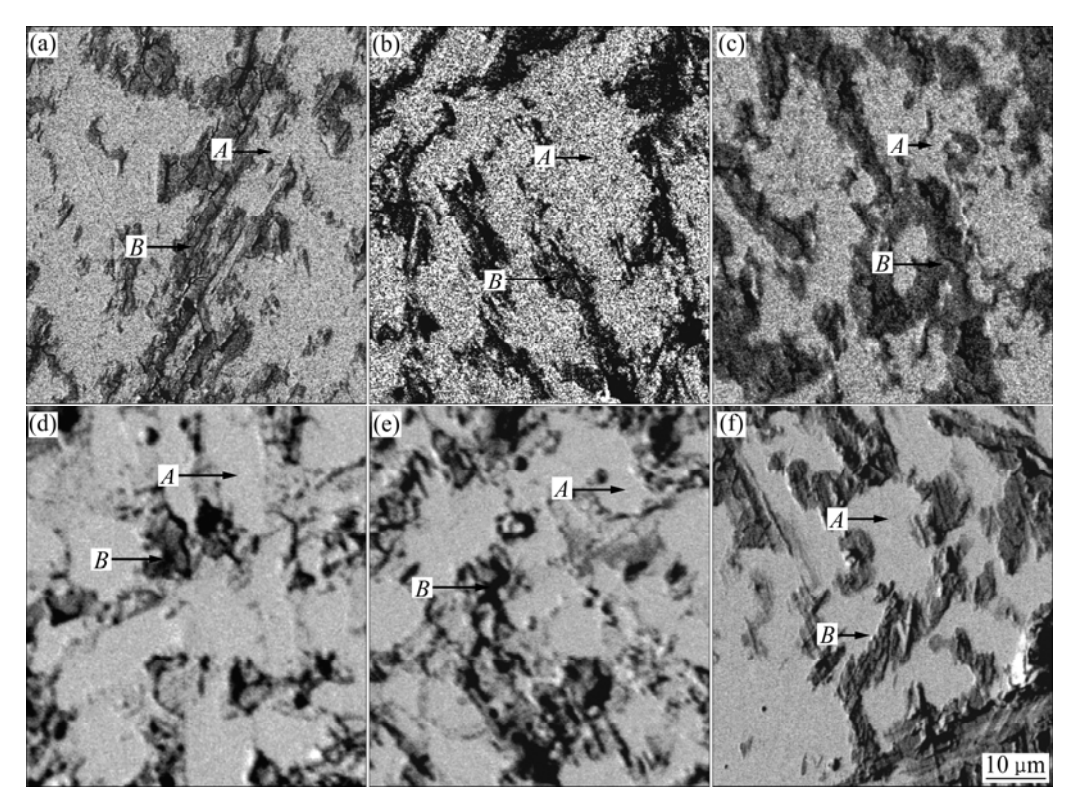
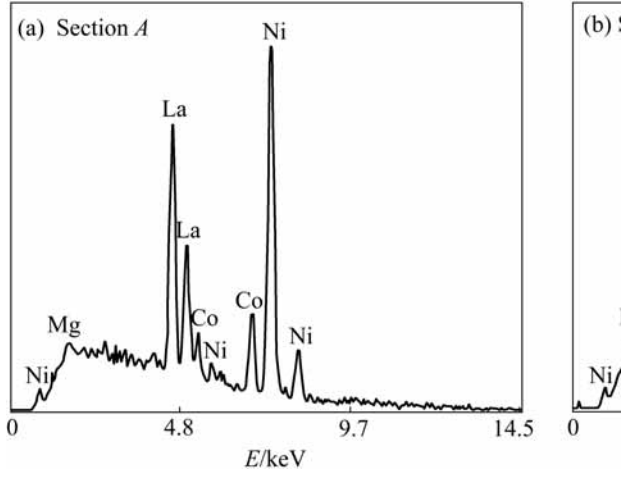


Fig.2 SEM images of La_{0.75}Mg_{0.25}Ni_{3.5}M_x alloys: (a), (b) and (c) M = Ni, x=0.2, 0.4 and 0.6; (d), (e) and (f) M=Co, x=0.2, 0.4 and 0.6, respectively



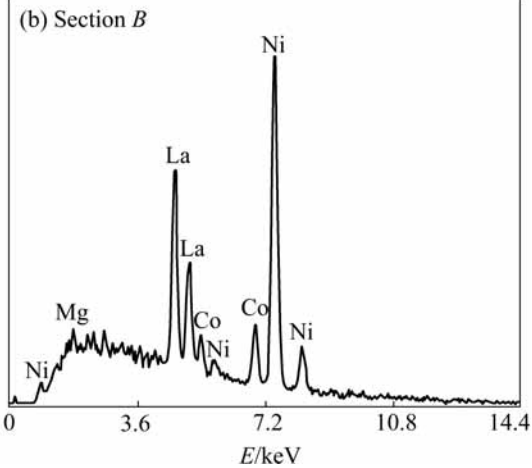


Fig.3 Typical EDS spectra of sections A and B in Fig.2(d)

the alloy (B/A - 3.7) rises with increasing B/A ratio, but the increase of B/A ratio (B/A > 3.7) leads to the decrease of the discharge potential of the alloy; and for the alloy (M=Co), the discharge potential of the alloy rises with the increase of B/A ratio. The plateau potential is closely relative to the internal resistance of the battery, including ohmic internal resistance and polarization resistance. The discharge reaction of the alloy electrode mainly depends on the diffusion of hydrogen atoms in the alloy, and the internal resistance of the alloy electrode reduces with the increase of the diffusion coefficient of the hydrogen

atom[5]. A proper ratio of $(La,Mg)_2Ni_7$ to $LaNi_5$ phases is probably the reason why the alloy (B/A=3.7) has a high discharge potential.

The maximum discharge capacities of the La_{0.75}Mg_{0.25}Ni_{3.5}M_x (M=Ni, Co; x=00.6) alloys as a function of B/A ratio are shown in Fig.5, at charge-discharge current density being 60 mA/g. It can be derived from Fig.5 that the discharge capacity increases from 343.7 (x=0) to 365.7 mA·h/g (x=0.2), and then drops to 311.2 mA·h/g (x=0.6) for the alloys (M=Ni); and for the alloys (M=Co), it mounts up from 343.7 (x=0) to

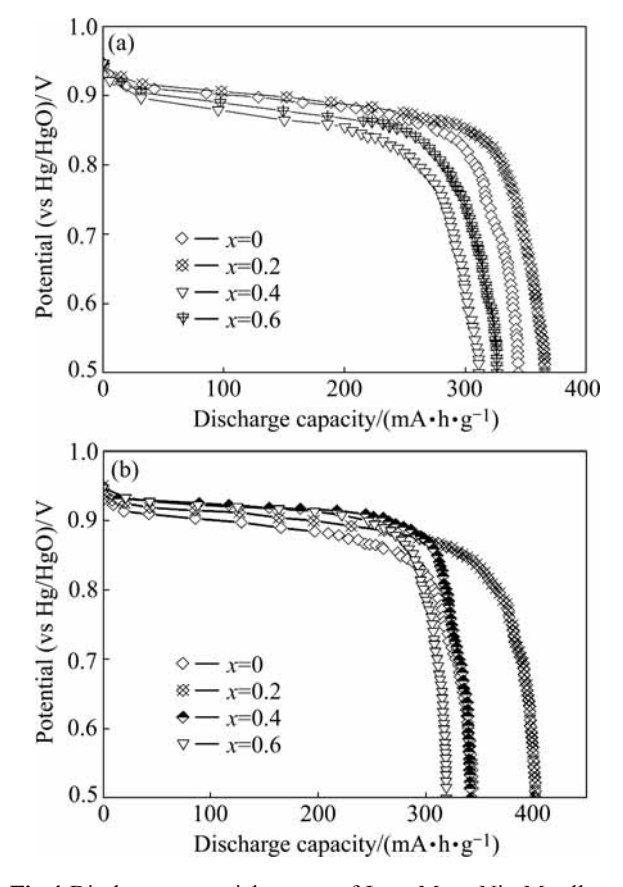


Fig.4 Discharge potential curves of La_{0.75}Mg_{0.25}Ni_{3.5}M_x alloys: (a) M=Ni; (b) M=Co

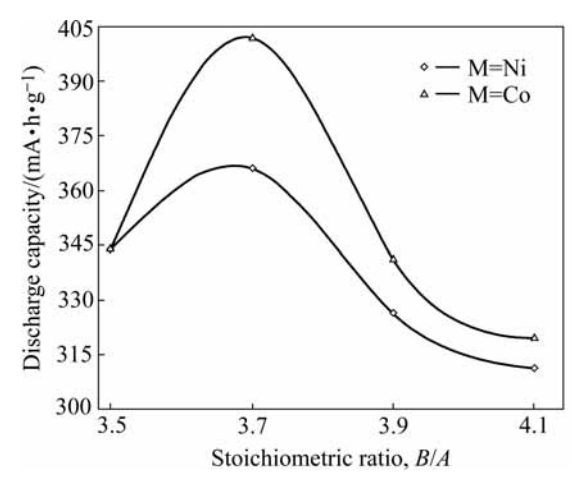


Fig.5 B/A ratio dependence of discharge capacities of $La_{0.75}Mg_{0.25}Ni_{3.5}M_x$ alloys

401.8 mA·h/g (x=0.2), and then declines to 319.2 mA·h/g (x=0.6). It is also seen in Fig.5 that for a fixed B/A ratio, the substitution of Co for Ni significantly enhances the discharge capacity of the alloy. The maximum discharge capacities of the alloys first increase and then decrease with increasing B/A ratio and the alloys obtain their maximum discharge capacities when ratio B/A=3.7, which is relevant to the change of the phase abundances of the alloys caused by the variety of B/A ratio. The

LaNi₅ phase in the alloy increases with rising B/A ratio (Fig.1), which is disadvantageous to the discharge capacity of the alloy due to the fact that the discharge capacity of the LaNi₅ phase is less than that of the (La,Mg)Ni₃ phase[6–7]. However, it is noteworthy that the LaNi₅ phase works not only as a hydrogen reservoir but also as a catalyst to activate the (La,Mg)₂Ni₇ phase to absorb/desorb reversibly hydrogen in the alkaline electrolyte[8–9]. It is the above contrary effect that results in an optimum B/A ratio for the discharge capacity of the alloy. The fact that Co substitution raises the discharge capacity of the alloys is mainly attributed to the increase of the cell volumes of the alloy caused by the substitution.

3.2.2 High rate discharge(HRD) capability

The high rate discharge(HRD) capability, a kinetic property of the alloy electrode, is calculated according to the following formula:

$$HRD = \frac{C_{600}}{C_{600} + C_{60}} \times 100\% \tag{1}$$

where C_{600} is the discharge capacity at a discharge current density of 600 mA/g at the cut-off potential of -0.500 V (vs Hg/HgO reference electrode), C_{60} is the residual discharge capacity at a discharge current density of 60 mA/g also at the cut-off potential of -0.500 V (vs Hg/HgO reference electrode) after the alloy electrode has been fully activated at a discharge current density of 60 mA/g. The HRD capabilities of the $La_{0.75}Mg_{0.25}Ni_{3.5}M_x$ (M=Ni, Co; x=0-0.6) alloys as a function of B/A ratio are shown in Fig.6. It can be derived from Fig.6 that when B/A ratio increases from 3.5 to 4.1, the HRD capability grows from 82.6% (B/A=3.5) to 89.97% (B/A=4.1) for the alloy (M=Ni), and it mounts up from 82.6% (B/A=3.5) to 90.69% (B/A=3.7), and then drops to 78.74% (B/A=4.1) for alloy (M=Co). The HRD capability of the alloy (M=Ni) monotonously rises with growing B/A ratio, for which the increase of the LaNi₅ phase is mainly respon-

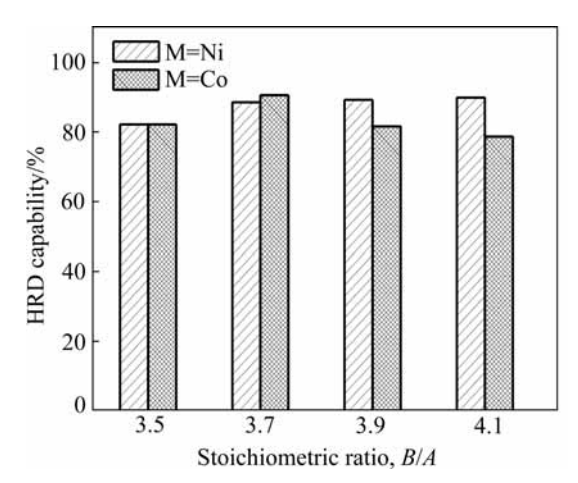


Fig.6 B/A ratio dependence of high rate discharge capabilities (HRDs) of La_{0.75}Mg_{0.25}Ni_{3.5}M_x alloys

sible because the LaNi₅ phase has a good electrocatalytic activity. The substitution of Co for Ni enhances the HRD capability of the alloy (B/A)3.7), which may be ascribed to the fact that the moderate substitution of Ni by Co can cause the concentration of Co and Ni at the surface of the alloy particles during charge/discharge cycling and the formation of Raney Ni-Co film with higher electrocatalytic activity[10-11]. However, with the further increase of B/A ratio, the substitution of Co for Ni leads to a slight decrease of the HRD capability of the alloy, which can be attributed to the decrease in effective surface area as a result of the decreased volume expansion[12] and the decrease in electrocatalytic activity because of the notable reduction of the Ni content due to the increase of Co substitution.

The electrochemical impedance spectra(EIS) were measured in the KOH electrolyte at 303 K. Fig.7 shows the typical electrochemical impedance spectra(EIS) of the $La_{0.75}Mg_{0.25}Ni_{3.5}M_x$ (M=Ni, Co; x=0-0.6) alloy electrodes at 50% depth of discharge(DOD) and 303 K, displaying that the EIS of all the alloys consist of two semicircles. The larger semicircle in the low-frequency region in the spectra can be characterized as the reaction resistance in the charge-transfer process[13]. As shown

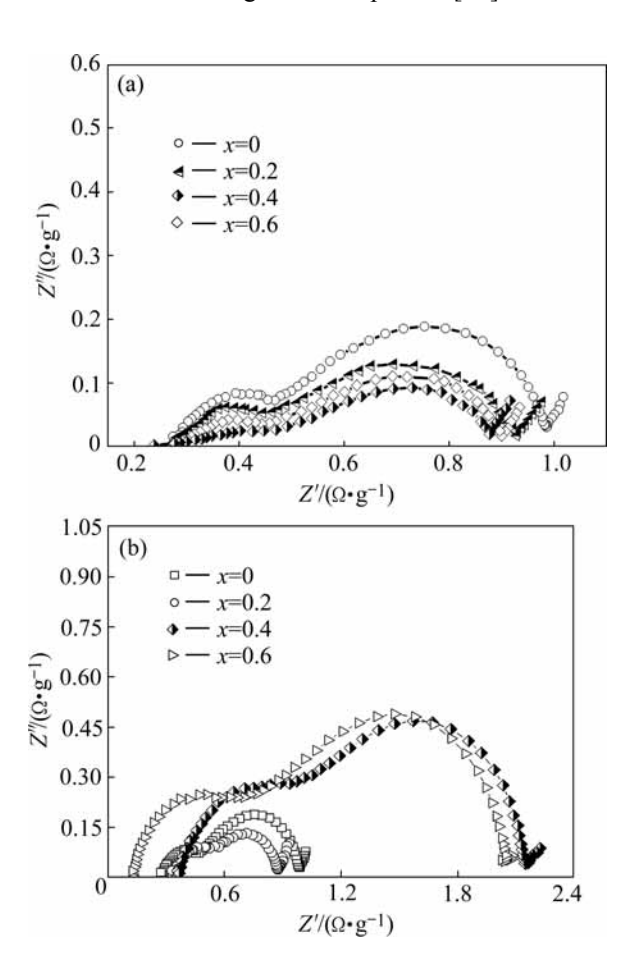


Fig.7 Electrochemical impedance spectra of $La_{0.75}Mg_{0.25}Ni_{3.5}-M_x$ alloy electrodes measured at 50% depth of discharge and 303 K: (a) M=Ni, (b) M=Co

in Fig.7, the radius of the larger semicircle in the low-frequency region reduces with increasing B/A ratio for the alloy (M=Ni), but it first reduces and then enlarges when Co content x increases from 0 to 0.6, suggesting that the increase of Ni content decreases the charge-transfer reaction resistance of the alloy electrode, but the increase of Co content leads to the charge-transfer reaction resistance to first decrease and then increase, which is in good agreement with the HRD capabilities of the alloys.

3.2.3 Cycle stability

The cycle stability of the alloys, characterized by the capacity retaining rate (S_{100}) , is defined as S_{100} = (C_{100}/C_{max}) × 100%, where C_{max} is the maximum discharge capacity, and C_{100} is the discharge capacity of the 100th cycle at a current density of 600 mA/g, respectively. The B/A ratio dependence of the capacity retaining rate (S_{100}) of the La_{0.75}Mg_{0.25}Ni_{3.5}M_x (M=Ni, Co; x=0-0.6) alloys is plotted in Fig.8. The figure shows that when B/A ratio rises from 3.5 to 4.1, the capacity retaining rate (S_{100}) drops from 51.5% (B/A=3.5) to 50.32% (B/A=3.7) and then mounts up to 55.53% (B/A= 4.1) for the alloy (M=Ni), and it enhances from 51.5% (B/A=3.5) to 60.09% (B/A=4.1) for the alloy (M=Co). It can be clearly seen in Fig. 8 that for a fixed B/A ratio, the Co substitution raises the capacity retaining rate (S_{100}) of the alloy.

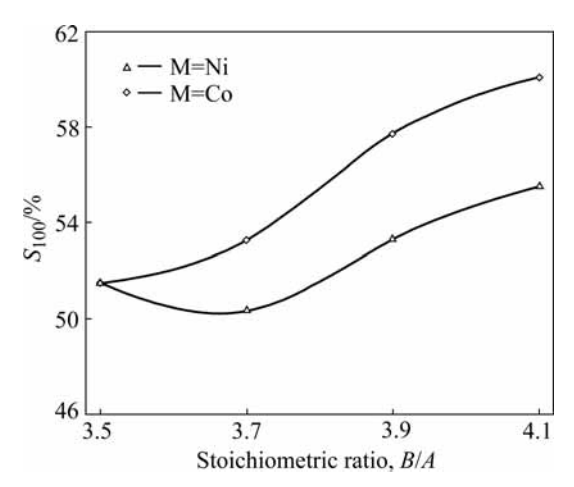


Fig.8 B/A ratio dependence of capacity retaining rate (S_{100}) of alloys

In order to understand correctly the mechanism of the efficacy loss of the experimental alloy electrode, the morphologies of the alloy particles before and after electrochemical cycle observed by SEM are shown in Fig.9. The cracks on the surface of the alloy particles after electrochemical cycle can clearly be seen in Fig.9(b), confirming that the pulverization of alloy particles takes place in the process of charging-discharging cycle, but the pulverization degree of the alloy is much smaller than that of the AB₅-type alloy[14].

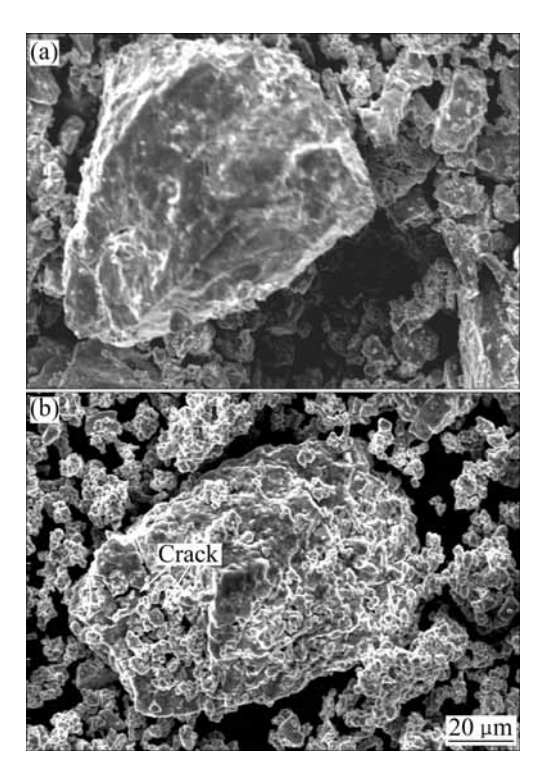


Fig.9 SEM morphologies of alloy (x=0) before (a) and after (b) electrochemical cycle

It is noteworthy that a rough and porous layer can clearly be found on the surface of the alloy particles after electrochemical cycle.

In order to confirm the presence of the oxidation layer on the surface of the alloy electrode, the core level spectra of La3d and Mg2p orbital electrons in the alloy (x=0) before and after electrochemical cycling are analyzed, as shown in Fig.10. The deviation of these peaks caused by the charge effect is corrected by binding energy (284.6 eV) for C1s, using a software of XPSEAK, obtaining the binding energies of La3d and Mg2p orbital electrons. The level binding energies of La3d and Mg2p orbital electrons are 835.90 and 49.8 eV, respectively, showing that the electrochemical cycle leads to an obvious change of the binding energies of La 3d and Mg 2p orbital electrons. The binding energy of Mg 2p from energy spectra before cycling exceeds that of metallic Mg (49.8 eV), which is ascribed to the oxidization of Mg owing to its contacting with air, as shown in the Fig.10(a). Therefore, it can be concluded that the reason why electrochemical cycle causes a change of the binding energies of the alloy electrons is that La and Mg in the alloy are oxidized to form La₂O₃ and MgO because La and Mg directly contact with the

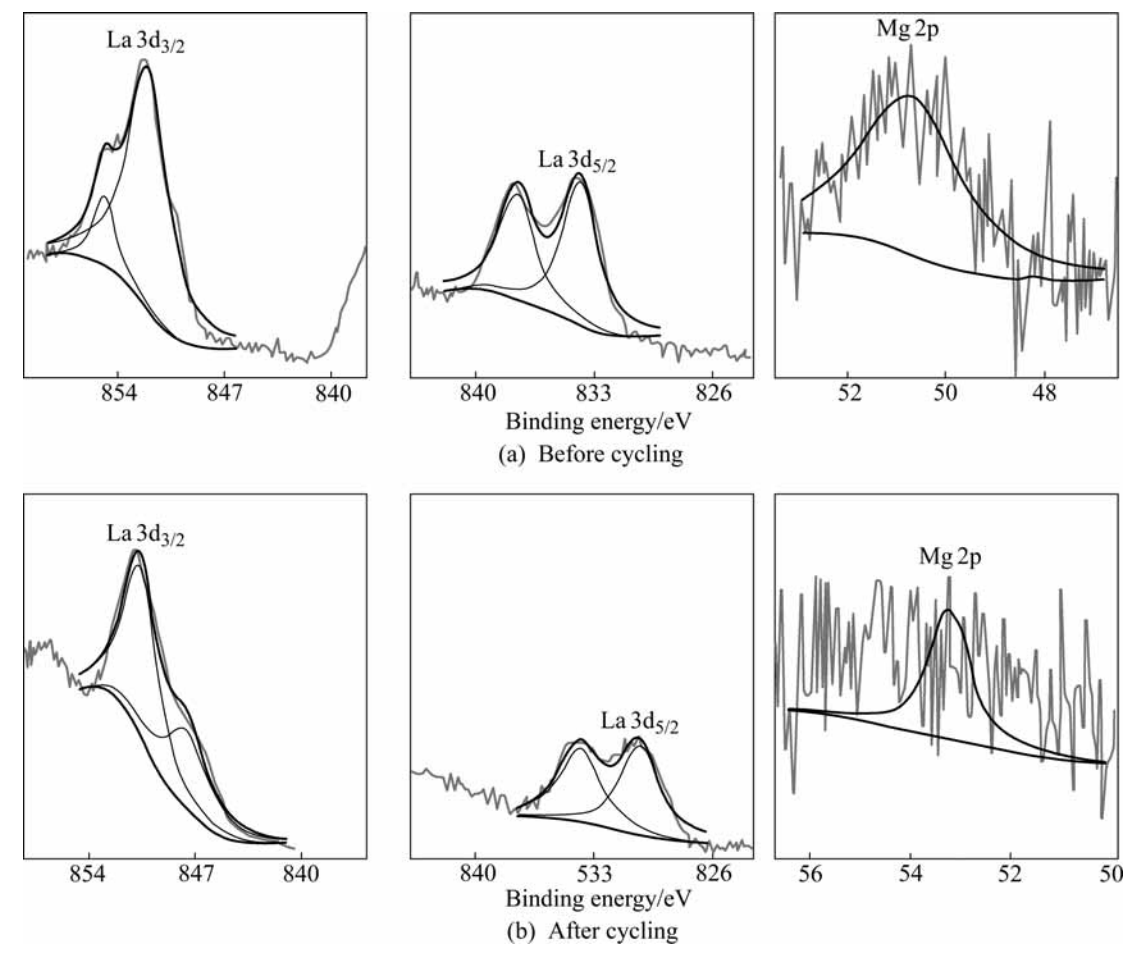


Fig.10 Core level spectra of La 3d and Mg 2p orbital electrons in alloy (x=0) before and after electrochemical cycle

alkaline electrolyte during electrochemical cycle. It is the oxidation-passivation layer, decreasing the electronic conductibility of the surface of the alloy electrode, preventing the diffusion of hydrogen atoms, reducing charge-transfer in the process of electrochemical reaction, that lessens the capability of hydrogen absorption/desorption of the alloy.

The positive impact of the Co substitution on the cycle stability is ascribed to the increase of the cell volume and the decrease of the expansion/contraction ratio of the alloy in the process of the hydrogen absorption/desorption, which means strengthening the anti-pulverization capability of the alloy.

4 Conclusions

- 1) The La-Mg-Ni-Co system La_{0.75}Mg_{0.25}Ni_{3.5}M_x (M=Ni, Co; x= 0, 0.2, 0.4, 0.6) hydrogen storage alloys have a multi-phase structure, involving the (La,Mg)₂Ni₇ and LaNi₅ major phases as well as the LaNi₂ residual phase. When B/A ratio increases from 3.5 to 4.1, the content of (La,Mg)₂Ni₇ phase reduces from 74.68% to 28.53%, and that of the LaNi₅ phase grows from 23.04% to 71.42% for the alloy (M=Ni), and from 74.68% to 31.06% and from 23.04% to 68.91% for the alloy (M=Co), respectively.
- 2) The discharge capacities of the alloys have a maximum value with the variety of B/A ratio. The HRD capability of the alloy (M=Ni) monotonously rises with growing B/A ratio, but the HRD capability of the alloy (M=Co) first rises and then drops. The capacity retaining rates (S_{100}) of the alloy (M=Ni) first decrease then increase with the incremental change of B/A ratio, whereas the rates of the alloy (M=Co) monotonously increase.
- 3) The substitution of Co for Ni significantly affects the electrochemical performances of the alloys: enhancing the discharge capacity and the cycle stability, improving the discharge potential characteristic, increasing the high rate discharge (HRD) ability of the alloys (B/A 3.7).
- 4) When the stoichiometric ratio B/A is 3.7, the alloys exhibit good integrative electrochemical performances: the discharge capacity of 343.7 mA·h/g, the high rate discharge(HRD) ability of 88.65%, the capacity retaining rate (S_{100}) of 50.32% for the alloy (M=Ni), and 401.8 mA·h/g, 90.69% and 53.26% for the alloy (M=Co), respectively.

References

- [1] LIU Y F, PAN H G, GAO M X, LEI Y Q, WANG Q D. XRD study on the electrochemical hydriding/dehydriding behavior of the La-Mg-Ni-Co-type hydrogen storage alloys [J]. J Alloys Comp, 2005, 403: 296–304.
- [2] KOHNO T, YOSHIDA H, KAWASHIMA F, INABA T, SAKAI I, YAMAMOTO M, KANDA M. Hydrogen storage properties of new ternary system alloys: La₂MgNi₉, La₅Mg₂Ni₂₃, La₃MgNi₁₄ [J]. J Alloys Comp, 2000, 311: L5–L7.
- [3] PAN H G, LIU Y F, GAO M X, ZHU Y F, LEI Y Q, WANG Q D. An investigation on the structural and electrochemical properties of La_{0.7}Mg_{0.3}(Ni_{0.85}Co_{0.15})_x (x=3.15-3.80) hydrogen storage electrode alloys [J]. J Alloys Comp, 2003, 351: 228-234.
- [4] WANG D H, LUO Y C, YAN R X, ZHANG F L, KANG L. Phase structure and electrochemical properties of La_{0.67}Mg_{0.33}Ni_{3.0-x}Co_x (x=0, 0.25, 0.5, 0.75) hydrogen storage alloys [J]. J Alloys Comp, 2006, 413: 193–197.
- [5] LAI W H, YU C Z. Research survey of improving discharge voltage platform for Ni-MH battery [J]. Chinese Battery, 1996, 26(4): 189–191. (in Chinese)
- [6] LIU Y F, PAN H G, GAO M X, ZHU Y F, LEI Y Q. Hydrogen storage and electrochemical properties of the La_{0.7}Mg_{0.3}Ni_{3.825-x}-Co_{0.675}Mn_x hydrogen storage electrode alloys [J]. J Alloys Comp, 2004, 365: 246–252.
- [7] TAKESHITA T, WALLACE W E, CRAIG R S. Hydrogen solubility in 1:5 compounds between yttrium or thorium and nickel or cobalt [J]. Inorg Chem, 1974, 13: 2282–2283.
- [8] PAN H G, LIU Y F, GAO M X, LEI Y Q, WANG Q D. A study of the structural and electrochemical properties of La_{0.7}Mg_{0.3}-(Ni_{0.85}Co_{0.15})_x (x=2.5-5.0) hydrogen storage alloys [J]. J Electrochem Soc, 2003, 150(5): A565–A570.
- [9] LIU Y F, PAN H G, GAO M X, ZHU Y F, GE H W, LI S Q, LEI Y Q. Investigation on the structure and electrochemical properties of the rare-earth Mg-based hydrogen storage electrode alloys [J]. Acta Metallurgica Sinica, 2003, 39(6): 666–672. (in Chinese)
- [10] FIORINO M E, OPILA R L, KONSTADINIDAS K, FANG W C. Electrochemical and X-ray photoelectron spectroscopy characterization of surface films on MmNi_{3.5}Al_{0.8}Co_{0.7} [J]. J Electrochem Soc, 1996, 143: 2422–2428.
- [11] IWAKURA C, FUKUDA K, SENOH H, INOUE H, MATSUOKA M, YAMAMOTO Y. Electrochemical characterization of MmNi_{4.0-x}Mn_{0.75}Al_{0.25}Co_x electrodes as a function of cobalt content [J]. Electrochim Acta, 1998, 43: 2041–2046.
- [12] CHOQUETTE Y, MENARD H, BROSSARD L. Electrocatalytic performance of composite-coated electrodes for alkaline water electrolysis [J]. Int J Hydrogen Energy, 1990, 15: 21–26.
- [13] KURIYAMA N, SAKAI T, MIYAMURA H, UEHARA I, ISHIKAWA H, IWASAKI T. Electrochemical impedance and deterioration behavior of metal hydride electrodes [J]. J Alloys Comp, 1993, 202: 183–197.
- [14] ZHANG Y H, WANG G Q, DONG X P, GUO S H, REN J Y, WANG X L. Effect of substituting Co with Fe on the cycle stabilities of the as-cast and quenched AB₅-type hydrogen storage alloys [J]. J Power Sources, 2005, 148: 105–111.

(Edited by YUAN Sai-qian)